ChemComm

Aqueous light-driven hydrogen production by a Ru-Ferredoxin-Co biohybrid

Journal:	*ChemComm*
Manuscript ID:	CC-COM-04-2015-003006.R2
Article Type:	Communication
Date Submitted by the Author:	28-May-2015
Complete List of Authors:	Soltau, Sarah; Argonne National Laboratory, Chemical Sciences and Engineering Division Niklas, Jens; Argonne National Laboratory, Chemical Sciences & Engineering Dahlberg, Peter; University of Chicago, Graduate program in biophysical sciences Poluektov, O. G.; Argonne National Laboratory, Chemical Sciences and Engineering Division Tiede, David M; Chemical Sciences + Engineering Division Argonne National Laboratory Building 20, Mulfort, Karen; Argonne National Laboratory, Chemical Sciences and Engineering Division Utschig, Lisa; Argonne National Laboratory, Chemical Sciences and Engineering Division

ChemComm

COMMUNICATION

Aqueous light driven hydrogen production by a Ru-Ferredoxin-Co biohybrid

Received 00th January 20xx,
Accepted 00th January 20xx

DOI: 10.1039/x0xx00000x

www.rsc.org/

S. R. Soltau,[a] J. Niklas,[a] P. D. Dahlberg,[a,b] O. G. Poluektov,[a] D. M. Tiede,[a] K. L. Mulfort,[a] and L. M. Utschig[a]*

Herein we report the creation of a novel solar fuel biohybrid for light-driven H_2 production utilizing the native electron transfer protein ferredoxin (Fd) as a scaffold for binding of a ruthenium photosensitizer (PS) and a molecular cobaloxime catalyst (Co). EPR and transient optical experiments provide direct evidence of a long-lived (>1.5 ms) Ru(III)-Fd-Co(I) charge separated state formed via an electron relay through the Fd [2Fe-2S] cluster, initiating the catalytic cycle for $2H^+ + 2e^- \rightarrow H_2$.

Sunlight is a powerful renewable energy source, however new materials are required to capture and convert this energy into usable fuels. Storing solar energy in chemical bonds, such as that in hydrogen, provides a robust source of fuel.[1] Protein-based approaches to solar fuels using molecular catalysts have been of growing interest. Notable examples include cobalt and iron catalysts attached to peptides,[2] an Fe-Fe hydrogenase mimic inserted into the heme pocket of cytochrome c[3] or to the external edge of nitrobindin,[4] and cobalt porphyrin[5] and cobaloxime[6] catalysts bound to myoglobin. Photocatalytic studies of these systems use freely diffusing photosensitizer (PS), $[Ru(bpy)_3]^{2+}$, and protein-bound catalyst to produce hydrogen.[2-6] Both PS and catalyst have been linked to one peptide structure, however low catalytic efficiency was observed.[7] Recently our laboratory has developed solar fuel hybrids that use the optimized photochemistry of a photosynthetic reaction center protein, Photosystem I (PSI), in lieu of a synthetic PS, to drive light-induced H_2 production from protein bound cobaloxime[8] and Ni diphosphine[9] catalysts. Additionally, we developed a strategy for inserting the Ni diphosphine catalyst non-covalently within the native cofactor binding pocket of a flavodoxin protein for H_2 generation; stabilizing the molecular catalyst which, in the absence of the protein environment, has low solubility and rapidly degrades in water.[9]

Ultimately, further development of protein-based hybrid as well as homogeneous synthetic multi-[10] and supramolecular[11] photocatalytic systems relies on understanding essential mechanisms for coupling captured photons to fuel generation. Although PSI-based hybrids rapidly produce H_2 from water,[12] PSI's large size (~350 kDa) and multiple spectroscopically overlapping terminal cofactors (3 [4Fe-4S] clusters) prevent the direct observation of light-driven electron transfer between PSI and the molecular catalyst. For this reason, we have targeted the development of a mini reaction center/catalyst hybrid that will enable the spectroscopic characterization and monitoring of dynamic light-induced catalytic intermediates for $2H^+ + 2e^- \rightarrow H_2$. Our design strategy involves a small (10.5 kDa) soluble electron transfer protein, *Spinacia oleracea* ferredoxin (Fd), as a scaffold for a controlled linkage of a Ru PS and a cobaloxime catalyst (Fig. 1A), thereby mimicking supramolecular donor-acceptor systems while incorporating important reaction center design attributes of an intermediary protein environment and electron acceptor cofactor.

The cobaloxime catalyst used in this study (Fig. 1B) covalently binds with Fd upon mixing. Metal binding analysis by ICP-AES following removal of unbound catalyst by microfiltration indicates 1.1 ± 0.4 Co/Fd. The Co catalyst is proposed to form an axial ligand to His 90 of Fd (verified by EPR analysis, Fig. 2). The Ru PS (Fig. 1C) performs bromine substitution reactions of cysteine thiols[13] and forms a covalent thiolate linkage with Cys18, directly connecting the protein and PS. The incorporation of Ru is lower (0.4 ± 0.2 Ru/Fd by ICP-AES); surface mapping of Fd suggests that Cys 18 is more buried within the protein than His 90, restricting direct access of the Ru PS to the Cys residue (Fig. S1). Modification of Cys18 with 5,5′-dithio-bis(2-nitrobenzoic acid) indicates one free Cys/Fd and the modified protein is unreactive to subsequent binding of the Ru PS. The distances from the Ru PS to the [2Fe-2S] cluster to the Co catalyst are all 12-15 Å, which should facilitate electron transfer among the three redox active species.

[a] Chemical Sciences and Engineering Division, Argonne National Laboratory, Argonne, IL 60439, USA, Email: utschig@anl.gov; Tel: +1-630-252-3544
[b] Graduate Program in Biophysics, The University of Chicago, Chicago, IL 60637, USA

† Electronic Supplementary Information (ESI) available: Experimental methods, H_2 production and TA controls, additional EPR spectra, and EPR simulation parameters. See DOI: 10.1039/x0xx00000x

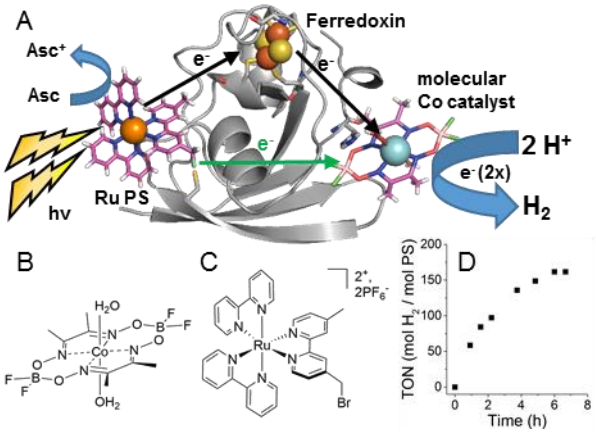

Figure 1. A) Photocatalytic H_2 production scheme in Ru-Fd-Co biohybrids with two potential pathways for electron transfer from PS to catalyst; via the [2Fe-2S] cluster of Fd (1A70), black arrows; directly from PS to catalyst, green arrow. B-C) Chemical structures of (B) cobaloxime catalyst (Co), $Co(dmgBF_2)_2{\cdot}2H_2O$ and (C) ruthenium photosensitizer (Ru PS), $[Ru(4\text{-}CH_2Br\text{-}4'\text{-}CH_3\text{-}2,2'\text{-}bpy)(bpy)_2]{\cdot}2PF_6$ used in the study. D) Representative time course profile of H_2 production from Ru-Fd-Co hybrid upon visible light illumination. The assay conditions are 2 µM Ru-Fd-Co hybrid (0.6 Ru/Fd, 0.9 Co/Fd) in 10 mM MES pH 6.3, 100 mM sodium ascorbate.

The Ru-Fd-Co complex produces hydrogen upon illumination with visible light (Fig. 1D). A variety of different buffer and pH conditions were investigated for optimal H_2 generation, as described in the ESI. The best conditions for photocatalysis with the Ru-Fd-Co hybrid are 10 mM MES buffer pH 6.3 with 100 mM sodium ascorbate as a sacrificial electron donor. The initial rate of H_2 production for the Ru-Fd-Co complex was 60 mol H_2(mol Ru PS)$^{-1}$ h^{-1} ([26 mol H_2(mol Fd)$^{-1}$ h^{-1}], turnover frequency) and H_2 production typically continues for 6-8 h. The maximum turnovers observed in 6 h was 320 mol H_2/mol Ru PS (130 mol H_2/mol Fd), with an average of 210 ± 60 turnovers/Ru PS (6 experiments). After hydrogen production ceased, the Ru-Fd-Co complex was washed to remove unbound metals and again analyzed by ICP-AES. Ru-Fd-Co complexes illuminated for 2-4 h retain metal binding with the same stoichiometry as before illumination, consistent with covalent bonding of PS and cobaloxime to Fd.

Notably, the Fd protein architecture facilitates H_2 production. Photocatalysis with 1 µM Co catalyst and 1 µM Ru PS (no Fd) yielded no detectable H_2 in these experiments (Table S1), presumably due to diffusion limitations. Additionally, the 320 turnovers obtained with our Ru-Fd-Co complex is much higher than the one other reported example of a linked Ru PS–molecular catalyst system, a peptide structure of cytochrome c with the Fe-Fe hydrogenase mimic, produced 9 turnovers.[7] Sperm-whale myoglobin bound to the same cobaloxime catalyst in this study can produce H_2 in the presence of excess $[Ru(bpy)_3]^{2+}$ and ascorbate, however, this system reached a maximum of 3.8 turnovers, and was suggested to be limited by structural confinement of the myoglobin binding cavity.[6]

To assess the importance of the [2Fe-2S] cluster of Fd in the function of the hybrid, we prepared the Ru-ApoFd-Co complex by removal of the [2Fe-2S] cluster via trichloroacetic acid precipitation.[9] Suspension of the protein pellet with the Ru PS yields a hybrid with <0.1 Fe/ApoFd. Co addition to the complex by self-assembly yields a complete Ru-ApoFd-Co hybrid with similar Ru and lower Co incorporation than the native hybrid (0.4 ± 0.1 Co/ApoFd, 0.3 ± 0.1 Ru/ApoFd). Upon illumination under the same conditions as the native complex, the apo-complex does not produce any detectable H_2. Optimization of reaction conditions for the Ru-ApoFd-Co hybrid was attempted, but no measureable H_2 production was observed after numerous trials. This result shows that H_2 formation relies on the [2Fe-2S] cluster, suggesting that one or two of the photoinduced electron transfers from Ru PS to the Co catalyst proceeds thru the [2Fe-2S] pathway (Fig. 1A).

The Co binding site in Fd was characterized with electron paramagnetic resonance (EPR) studies (Fig. 2). The Co catalyst studied herein has a resting EPR active $3d^7$ low spin Co(II) oxidation state,[14] and is sensitive to oxygen versus nitrogen axial coordination.[15] The Fd-Co hybrid in the dark (Fig. 2A, black) has a very weak Co(II) signal, suggesting that most of the initial complex forms a Co(III) species, which has been previously observed for this Co catalyst bound to myoglobin.[6] After addition of ascorbate, we observed a strong Co(II) signal confirming reduction of the Co catalyst (Fig. 2A, red). The spectrum of the Co catalyst in buffer (Fig. 2A, blue) was subtracted from the spectrum of Fd-Co with ascorbate; the resulting spectrum (Fig. 2A, green) has a line shape characteristic for a cobaloxime complex with single N-coordination (simulation of the nitrogen coordinated Fd-Co spectrum, Fig. S2 dashed green, simulation parameters, Fig. S3).[15] Approximately 70% of Co is N-coordinated and 30% is O-coordinated while the exact type of ligand cannot be determined. We hypothesize that the 70% N-coordinated Co is specifically bound to His 90, but multiple surface aspartate and glutamate residues likely compete for axial ligation to the cobaloxime. The g-values and hyperfine coupling of the N-

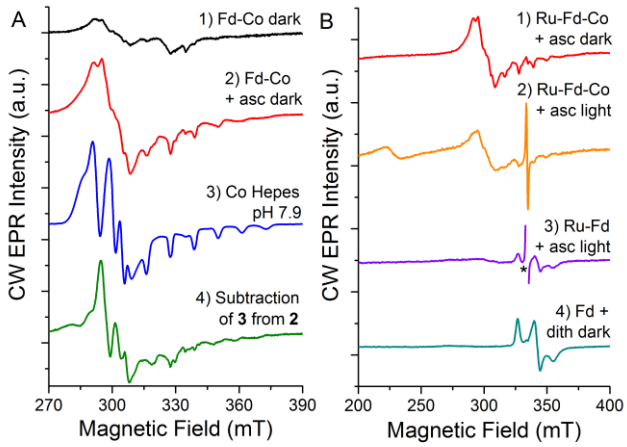

Figure 2. X-band cw EPR spectra of Fd-Co, Ru-Fd-Co, and Ru-Fd biohybrids. (A) Fd-Co dark (black, 1), Fd-Co dark + asc (red, 2), Co in Hepes buffer pH 7.9 (blue, 3), and subtraction of 3 from 2 to give representative spectra of N-coordination of Co in Fd-Co hybrids (green, 4). (B) Ru-Fd-Co + ascorbate dark (red, 1), Ru-Fd-Co + ascorbate light (orange, 2), Ru-Fd + ascorbate light (violet, 3), and Fd + dithionite dark (dark cyan, 4). "Light" samples were illuminated for 2 s at room temperature followed by immersion in liquid N_2 while illuminated and then placed in a pre-cooled EPR cavity for measurement. All EPR spectra were obtained at 10 K. An asterisk marks an organic radical omitted for clarity.

coordinated Co (g_x, 2.250; g_y, 2.158; g_z, 2.006; A_z, 280 MHz) agree with 1:1 Co : pyridine in methanol,[15] suggesting that the cobaloxime in the Fd-Co hybrid exists in a polar, buffer exposed environment consistent with ligation to the surface exposed His 90 (Fig. S1). This environment is quite distinct from the non-polar, hydrophobic surroundings suggested by the EPR parameters for the Co catalyst bound to the binding pocket of apo-myoglobin.[6]

In Ru-Co synthetic systems, electrons are transferred from PS to catalyst via an oxidative or reductive quenching mechanism.[16] EPR studies enable us to detect the involvement of these two mechanisms for our biohybrid complex. Like the Fd-Co hybrid, the Ru-Fd-Co hybrid exhibits a Co(II) signal in the presence of sodium ascorbate (Fig. 2B, red). Illumination of the reduced Ru-Fd-Co hybrid (Ru(II)-Fd-Co(II)) with freeze trapping techniques, leads to a 50% reduction in the Co(II) signal intensity, formation of a Ru(III) signal with g = 2.95 and an organic radical species (Fig. 2B, orange). A decrease in Co(II) signal intensity and appearance of Ru(III) signal is consistent with oxidative quenching of Ru(II)* and electron transfer to Co, forming an EPR silent Co(I) species. EPR signals of low spin d^5 Ru(III) complexes tend to form broad signals with g-values ~2.6-3.0.[17] A Ru(III) species (g = 2.90) was also observed in the absence of ascorbate for the Ru(II)-Fd-Co(III) hybrid following illumination; however this signal decayed within a minute (Fig. S4-S5).

An organic radical species is also observed in the ascorbate/illuminated Ru-Fd-Co and Ru-Fd hybrids (Fig. 2B, orange and violet), assigned to an ascorbate radical. This radical signal could either arise from incomplete reduction of Ru(III) generated by the oxidative quenching mechanism, or by a parallel reductive quenching pathway. We observed no evidence of Ru(I) formation, as Ru(I) species exhibit reduction of the ligands rather than metal centered radicals and would give higher field EPR signals.[18] Fd [2Fe-2S] cluster is detected by EPR when reduced.[19] Fig. 2B, dark cyan, shows the Fd EPR signal following reduction by sodium dithionite. After illumination, a Ru(II)-Fd hybrid in the presence of ascorbate generates a species with the same g-values as sodium dithionite reduced Fd (Fig. 2B, violet; g_x = 2.05, g_y = 1.96, g_z = 1.89). Thus, the Ru-Fd hybrid is capable of transferring electrons from Ru PS to the [2Fe-2S] cluster. This supports a primary mechanism of H_2 production which uses the [2Fe-2S] cluster to shuttle electrons to the Co catalyst.

To further examine the electron transfer processes in the biohybrids, transient optical spectroscopy was performed (Fig. 3). The Ru PS was excited with a laser pulse at 450 nm and kinetics were detected with a 660 nm LED, where the mechanistically relevant Co(I) species absorbs (Fig. S6-S8).[20] Additionally, Ru(II)* and Ru(III) absorb at 660 nm, although the absorption is weaker than Co(I) (Fig. S9).[21] Therefore, control experiments with $[Ru(bpy)_3]^{2+}$ were done to determine the contribution of Ru species to the spectra (Fig. 3A, inset and Fig. S10). Additional controls were performed in the presence of protein (Fig. S11). In contrast to the Ru control, the transient absorption for the Ru-Fd-Co hybrid shows evidence of a sub-µs

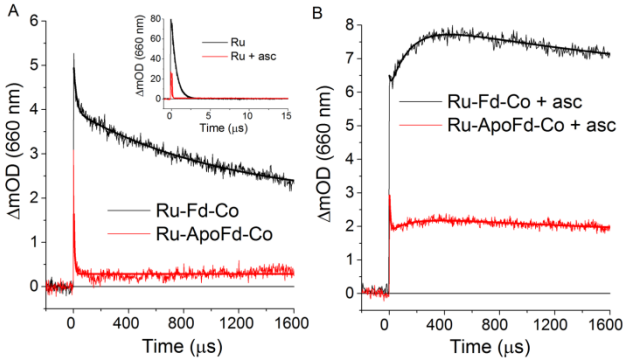

Figure 3. Transient optical kinetic traces at 660 nm where formation and decay of a Co(I) species is observed for the Fd hybrids. A) Ru-Fd-Co, black; Ru-ApoFd-Co, red. Inset: $[Ru(bpy)_3]^{2+}$, black; $[Ru(bpy)_3]^{2+}$ with 200 mM sodium ascorbate, red. B) Samples with 200 mM sodium ascorbate, Ru-Fd-Co, black; Ru-ApoFd-Co, red.

formation and long-lived (τ = 1.0 ± 0.1 ms) charge-separated state (Fig. 3A, black). The EPR results point to the identification of Ru(III)-Fd-Co(II) as the charge separated state, generated by oxidative quenching of Ru(II)* and electron transfer to the Co(III)-cobaloxime state observed in the absence of ascorbate. Strikingly, the Ru-ApoFd-Co hybrid (Fig. 3A, red) shows mainly fast, sub-microsecond Ru(II)* decay kinetics. Thus, Ru → Co electron transfer does not occur in the absence of the [2Fe-2S] cluster.

In the presence of ascorbate, the Ru(II)* excited state is quenched rapidly (~50 ns, Fig. 3A inset). Ru-Fd-Co + ascorbate (Fig. 3B, black) shows a sub-µs absorption rise and a long-lived (>1.5 ms) charge-separated state. The long-lived charge-separated state could arise from rapid Co(I) formation by oxidative quenching of Ru(II)*, as in Figure 3A and indicated by EPR, or by ascorbate reductive quenching of Ru(II)*. Similar to Ru-Fd-Co, the Ru-ApoFd-Co + ascorbate sample shows a sub-µs formation and a long-lived 660 nm absorption, suggestive of rapid formation of the Co(I) state, although with a 3x-4x smaller ΔOD (Fig. 3B, red). In both samples, an additional slow rise component (τ = 150 ± 10 µs) is observed which could result from Ru-Fd-Co in which the Co is not positioned for rapid electron transfer. The >1.5 ms lifetime of the Co(I) state is remarkable and is likely supported by the Fd protein matrix which prevents fast back charge recombination, thereby enabling efficient H_2 photocatalysis. In PSI-hybrids, the light-induced charge separated state of the primary donor, P700, and terminal acceptor, a [4Fe-4S] cluster, is long-lived (60 ms) and contributes to rapid H_2 photocatalysis, although the lifetimes of the Co(I) or Ni(I) catalytic intermediates have not been determined.[8-9] In comparison, supramolecular systems have short-lived Co(I) charge separated states due to fast back electron transfer thereby limiting H_2 production,[11b, 20] whereas accumulation of the Co(I) state has been observed in H_2 producing multimolecular systems.[22]

The transient optical absorption and EPR data lead us to propose a mechanism for H_2 production by the Ru-Fd-Co hybrids. This process proceeds through a Ru(III) species detected by EPR, which invokes an oxidative quenching mechanism for the Ru PS. In the proposed mechanism, light

excites $[Ru(bpy)_3]^{2+}$ to $[Ru(bpy)_3]^{2+}$* which can then transfer an electron either directly to the Co(II) resting catalyst or indirectly via Fd [2Fe-2S] cluster to form $[Ru(bpy)_3]^{3+}$ (Ru(II*/III) -0.8 V vs. NHE).[23] As evidenced by transient optical spectroscopy and null H_2 photocatalysis of Ru-ApoFd-Co, electron transfer via a [2Fe-2S] relay facilitates more efficient electron transfer to the Co(II) resting state and we believe this to be the primary electron transfer pathway (Figure 1A, black arrows). This is surprising due to the similar reduction potentials of the Fd [2Fe-2S] cluster (-0.42 V vs. NHE)[24] and Co(II/I) reduction potential of $Co(dmgBF_2)_2{\cdot}2H_2O$ in buffer (Co(II/I) -0.42 V vs. NHE (Figure S12)). The cobaloxime potential has not been determined in the protein environment. Following light-induced reduction, we expect that the Co(I) species ultimately abstracts a proton from the aqueous solution to form a Co(III)-hydride and performs subsequent proton coupled electron transfer to produce H_2 as has been proposed previously with cobaloximes.[25] The slow (>1.5 ms) decay of the Co(I) provides time for these reactions to occur. We further hypothesize that the [2Fe-2S] cluster aids in the photocatalysis mechanism, potentially providing a holding place for the second electron necessary for H_2 production. The catalytic cycle is regenerated by reduction of the oxidized PS with ascorbate as a sacrificial electron donor.

To summarize, we have developed a new functional biohybrid wherein the Fd protein matrix exhibits several design attributes of photosynthetic reaction center proteins; acting as a framework to (1) position Co catalyst and PS in close proximity, (2) stabilize charge separation, and (3) facilitate H_2 production via an electron relay through the native [2Fe-2S] cluster. This work establishes that protein environments provide a unique opportunity to develop scaffolds for solar fuel hybrids that extend beyond a small synthetic architecture and permit necessary catalyst flexibility and optimization for hydrogen or other solar fuel production.

This work is supported by the Division of Chemical Sciences, Geosciences, and Biosciences, Office of Basic Energy Sciences of the U.S. Department of Energy under Contract DE-AC02-06CH11357. This work was performed, in part (full TA spectra), at the Center for Nanoscale Materials, a U.S. Department of Energy, Office of Science, Office of Basic Energy Sciences User Facility under Contract No. DE-AC02-06CH11357.

Notes and references

1 (a) N. S. Lewis, *Science*, 2007, **315**, 798; (b) N. S. Lewis and D. G. Nocera, *Proc. Natl. Acad. Sci. U.S.A.*, 2006, **103**, 15729.
2 A. Roy, C. Madden and G. Ghirlanda, *Chem. Commun.*, 2012, **48**, 9816.
3 Y. Sano, A. Onoda and T. Hayashi, *Chem. Commun.*, 2011, **47**, 8229.
4 A. Onoda, Y. Kihara, K. Fukumoto, Y. Sano and T. Hayashi, *ACS Catal.*, 2014, **4**, 2645.
5 D. J. Sommer, M. D. Vaughn and G. Ghirlanda, *Chem. Commun.*, 2014, **50**, 15852.
6 M. Bacchi, G. Berggren, J. Niklas, E. Veinberg, M. W. Mara, M. L. Shelby, O. G. Poluektov, L. X. Chen, D. M. Tiede, C. Cavazza, M. J. Field, M. Fontecave and V. Artero, *Inorg. Chem.*, 2014, **53**, 8071.
7 Y. Sano, A. Onoda and T. Hayashi, *J. Inorg. Biochem.*, 2012, **108**, 159.
8 L. M. Utschig, S. C. Silver, K. L. Mulfort and D. M. Tiede, *J. Am. Chem. Soc.*, 2011, **133**, 16334.
9 S. C. Silver, J. Niklas, P. Du, O. G. Poluektov, D. M. Tiede and L. M. Utschig, *J. Am. Chem. Soc.*, 2013, **135**, 13246.
10 (a) J. L. Dempsey, B. S. Brunschwig, J. R. Winkler and H. B. Gray, *Acc. Chem. Res.*, 2009, **42**, 1995; (b) F. Lakadamyali, M. Kato, N. M. Muresan and E. Reisner, *Angew. Chem. Int. Ed.*, 2012, **51**, 9381.
11 (a) K. L. Mulfort, A. Mukherjee, O. Kokhan, P. W. Du and D. M. Tiede, *Chem. Soc. Rev.*, 2013, **42**, 2215; (b) A. Fihri, V. Artero, M. Razavet, C. Baffert, W. Leibl and M. Fontecave, *Angew. Chem. Int. Ed.*, 2008, **47**, 564.
12 L. M. Utschig, S. R. Soltau and D. M. Tiede, *Curr. Opin. Chem. Biol.*, 2015, **25**, 1.
13 J. Contzen, S. Kostka, R. Kraft and C. Jung, *J. Inorg. Biochem.*, 2002, **91**, 607.
14 A. Bakac, M. E. Brynildson and J. H. Espenson, *Inorg. Chem.*, 1986, **25**, 4108.
15 J. Niklas, K. L. Mardis, R. R. Rakhimov, K. L. Mulfort, D. M. Tiede and O. G. Poluektov, *J. Phys. Chem. B*, 2012, **116**, 2943.
16 (a) C. V. Krishnan and N. Sutin, *J. Am. Chem. Soc.*, 1981, **103**, 2141; (b) K. Kawano, K. Yamauchi and K. Sakai, *Chem. Commun.*, 2014, **50**, 9872.
17 (a) E. Sondaz, A. Gourdon, J. P. Launay and J. Bonvoisin, *Inorg. Chim. Acta.*, 2001, **316**, 79; (b) S. Sakaki, Y. Yanase, N. Hagiwara, T. Takeshita, H. Naganuma, A. Ohyoshi and K. Ohkubo, *J. Phys. Chem.*, 1982, **86**, 1038.
18 (a) R. M. Berger and D. R. Mcmillin, *Inorg. Chem.*, 1988, **27**, 4245; (b) A. G. Motten, K. Hanck and M. K. Dearmond, *Chem. Phys. Lett.*, 1981, **79**, 541.
19 R. E. Coffman and B. W. Stavens, *Biochem. Biophys. Res. Commun.*, 1970, **41**, 163.
20 A. Mukherjee, O. Kokhan, J. Huang, J. Niklas, L. X. Chen, D. M. Tiede and K. L. Mulfort, *Phys. Chem. Chem. Phys.*, 2013, **15**, 21070.
21 (a) L. A. Kelly and M. A. J. Rodgers, *J. Phys. Chem.*, 1994, **98**, 6377; (b) B. Shan, T. Baine, X. A. N. Ma, X. Zhao and R. H. Schmehl, *Inorg. Chem.*, 2013, **52**, 4853.
22 (a) R. S. Khnayzer, V. S. Thoi, M. Nippe, A. E. King, J. W. Jurss, K. A. El Roz, J. R. Long, C. J. Chang and F. N. Castellano, *Energy Environ. Sci.*, 2014, **7**, 1477; (b) A. Rodenberg, M. Orazietti, B. Probst, C. Bachmann, R. Alberto, K. K. Baldridge and P. Hamm, *Inorg. Chem.*, 2015, **54**, 646; (c) P. W. Du, J. Schneider, G. G. Luo, W. W. Brennessel and R. Eisenberg, *Inorg. Chem.*, 2009, **48**, 4952.
23 J. H. Alstrum-Acevedo, M. K. Brennaman and T. J. Meyer, *Inorg. Chem.*, 2005, **44**, 6802.
24 R. Cammack, K. K. Rao, C. P. Bargeron, K. G. Hutson, P. W. Andrew and L. J. Rogers, *Biochem J.*, 1977, **168**, 205.
25 (a) X. L. Hu, B. S. Brunschwig and J. C. Peters, *J. Am. Chem. Soc.*, 2007, **129**, 8988; (b) J. T. Muckerman and E. Fujita, *Chem. Commun.*, 2011, **47**, 12456; (c) B. H. Solis and S. Hammes-Schiffer, *J. Am. Chem. Soc.*, 2011, **133**, 19036.

